

# Scanning tunnelling microscopy observations at initial stage of Cs adsorption on Si(111)- $\sqrt{3} \times \sqrt{3}$ -Ag surface

Canhua Liu,\* Iwao Matsuda and Shuji Hasegawa

Department of Physics, School of Science, University of Tokyo, 7-3-1 Hongo, Bunkyo-ku, Tokyo 113-0033, Japan

Received 15 September 2003; Revised 18 December 2003; Accepted 20 January 2004

The growth and ordering behaviour of Cs adatoms at the initial stage of adsorption on the Si(111)- $\sqrt{3} \times \sqrt{3}$ -Ag surface have been investigated using low-temperature scanning tunnelling microscopy (STM). It was revealed that the Cs overlayer conducts two-dimensional gas–liquid–solid phase transitions by changing the Cs coverage below 0.143 monolayer. The STM images show that the Cs adatoms adsorb on a specific site in the unit cell of Si(111)- $\sqrt{3} \times \sqrt{3}$ -Ag structure and move around by hopping among the equivalent sites in the liquid state. As the coverage increases, the Cs adatoms condense into the solid state, forming the surface superstructure Si(111)- $\sqrt{21} \times \sqrt{21}$ -(Ag + Cs). Its atomic structure model was proposed based on STM observations. Copyright © 2005 John Wiley & Sons, Ltd.

**KEYWORDS:** gas; liquid; solid; scanning tunnelling microscopy; Si(111); two-dimensional

## INTRODUCTION

Matter exists in three thermodynamic states—gas, liquid and solid—depending on the temperature and pressure. In the gas state, matter has no order in atomic arrangement and the constituent atoms move around with high mobility; in the liquid state, matter possesses short-range order and the mobility of atoms becomes relatively much lower; in the solid state, a crystal displays long-range order in atomic arrangement and its constituent atoms have no mobility. Phase transitions among the three states have been long debated in physics,<sup>1</sup> especially for two-dimensional systems where the restricted degree of freedom brings about various exotic phenomena.<sup>2</sup>

Atomic overlayers on solid surfaces usually qualify as two-dimensional matter and have been utilized for studying two-dimensional phase transitions. Among them, alkali-metal atomic layers absorbed on metal and semiconductor surfaces have been studied intensively and have provided good test grounds for theoretical predictions. It was found that K atomic layers on Cu(111)<sup>3</sup> and Cu(001) surfaces<sup>4</sup> induce a two-dimensional liquid–solid phase transition, discovered in reciprocal space by low-energy electron diffraction (LEED). However, although the diffraction method provides short- and long-range orders of average atomic arrangements, it is necessary to obtain the local structure and inhomogeneity in atomic arrangement in real space by atomic resolution microscopy.

In the present study, by using scanning tunnelling microscopy (STM), we find that Cs adatoms adsorbed on the Si(111)- $\sqrt{3} \times \sqrt{3}$ -Ag ( $\sqrt{3}$ -Ag in short hereafter) surface

exhibit two-dimensional gas–liquid–solid phase transitions by changing the Cs coverage in the submonolayer range. The STM observations provide direct images of local atomic arrangements in real space and also the mobility of individual atoms.

The  $\sqrt{3}$ -Ag surface is used as the substrate in this study because it is atomically smooth without any dangling bonds, so the interaction between adatoms and substrate is known to be very weak.<sup>5,6</sup> This is an important requirement to prepare two-dimensional matter. Foreign atom adsorptions on the  $\sqrt{3}$ -Ag surface have been investigated quite widely so far.<sup>6</sup> In particular, the  $\sqrt{21} \times \sqrt{21}$  surface superstructures are known to appear by submonolayer adsorption of novel metals and alkali metals. For Cs adsorption on this surface, the Si(111)- $6 \times 6$ -(Ag + Cs) superstructure and the Si(111)- $\sqrt{21} \times \sqrt{21}$ -(Ag + Cs) ( $\sqrt{21}$ -Cs in short hereafter) superstructure are known to appear at around half a monolayer coverage.<sup>7</sup> The present study, on the other hand, focuses on much smaller amounts of Cs adsorption on the  $\sqrt{3}$ -Ag surface. Such a dilute overlayer of Cs adatoms has been found to be two-dimensional matter exhibiting two-dimensional gas–liquid–solid phase transitions by changing the Cs coverage, i.e. by changing the ‘pressure’.

## EXPERIMENTAL

All experiments, including sample preparation by Ag and Cs depositions on an Si crystal with the aid of reflection high-energy electron diffraction (RHEED) and STM observations (UNISOKU USM501), were carried out in an ultrahigh vacuum chamber. The base pressure was  $5 \times 10^{-11}$  Torr and the pressure was kept below  $3 \times 10^{-10}$  Torr during Cs and Ag evaporations. The Si(111) crystal was a B-doped p-type wafer with a resistivity of 2–10  $\Omega \cdot \text{cm}$  at room temperature and a size of  $15 \times 3 \times 0.4 \text{ mm}^3$ . It was flashed

\*Correspondence to: Canhua Liu, Department of Physics, School of Science, University of Tokyo, 7-3-1 Hongo, Bunkyo-ku, Tokyo 113-0033, Japan. E-mail: liu@surface.phys.s.u-tokyo.ac.jp

up to  $\sim 1200^\circ\text{C}$  by direct current flowing through the wafer after sufficient prolonged degassing at  $\sim 400^\circ\text{C}$ , resulting in a clean Si(111) $7 \times 7$  surface. The  $\sqrt{3}$ -Ag surface was prepared by evaporating Ag atoms of one monolayer (ML) from a basket onto this clean surface at a substrate temperature of  $\sim 520^\circ\text{C}$ . One ML here equals  $7.8 \times 10^{14}\text{cm}^{-2}$ , the density of the topmost Si atoms on the ideal Si(111) $1 \times 1$  surface. Both surface structures were confirmed by RHEED observations. After the crystal was cooled down to room temperature, very small but controlled amounts of Cs atoms were evaporated from a thoroughly outgassed commercial dispenser (SAES Getters Inc.) onto the  $\sqrt{3}$ -Ag surface. Then the sample was cooled down to 65 K by transferring it to a cold stage for low-temperature STM observations. The Cs coverage was determined directly from the STM images obtained, as explained in detail later.

## RESULTS AND DISCUSSION

Figure 1 shows STM images of the Cs-adsorbed  $\sqrt{3}$ -Ag surface at various Cs coverages, displaying the Cs overlayers in two-dimensional gas (a, b), liquid (c, d, e) and solid phases (f), respectively. Figures 1(a) and 1(b) are for the gas phase at a coverage of 0.01 ML, taken successively at an interval of  $\sim 100$  s on an identical area. There are many bright

protrusions randomly distributed on a terrace. Most of them display completely different positions in the two successive STM images. By continuing the STM scanning on the same area after these two images, we found that the positions of the bright protrusions kept changing, which indicates high mobility of the atoms. Because the protrusions were never observed on the pristine  $\sqrt{3}$ -Ag surface before Cs deposition, it is reasonable to assign the bright protrusions as Cs atoms. This is proved later. Thus, from Figs 1(a) and 1(b) we see that the Cs atoms (bright protrusions) exhibit high mobility and are arranged randomly. These facts indicate that the interaction between the Cs adatoms and the substrate is very weak and the overlayer of Cs atoms is qualified as two-dimensional matter in the gas state.

Increasing the Cs coverage makes the Cs overlayer condense into a two-dimensional liquid state from the gas state. Figures 1(c), 1(d) and 1(e) are STM images taken at the Cs coverage of 0.09 ML, successively imaged on an identical area at an interval of 150 s. As with those in Figs 1(a) and 1(b), the bright protrusions in Figs 1(c)–1(e) are all Cs adatoms. The density becomes much higher because the Cs coverage is increased by  $\sim 10$  times from that in Figs 1(a) and 1(b). The increase in Cs density makes the interactions among Cs atoms grow much stronger, so that they are arranged in short-range order. This is evidenced in the STM images by the

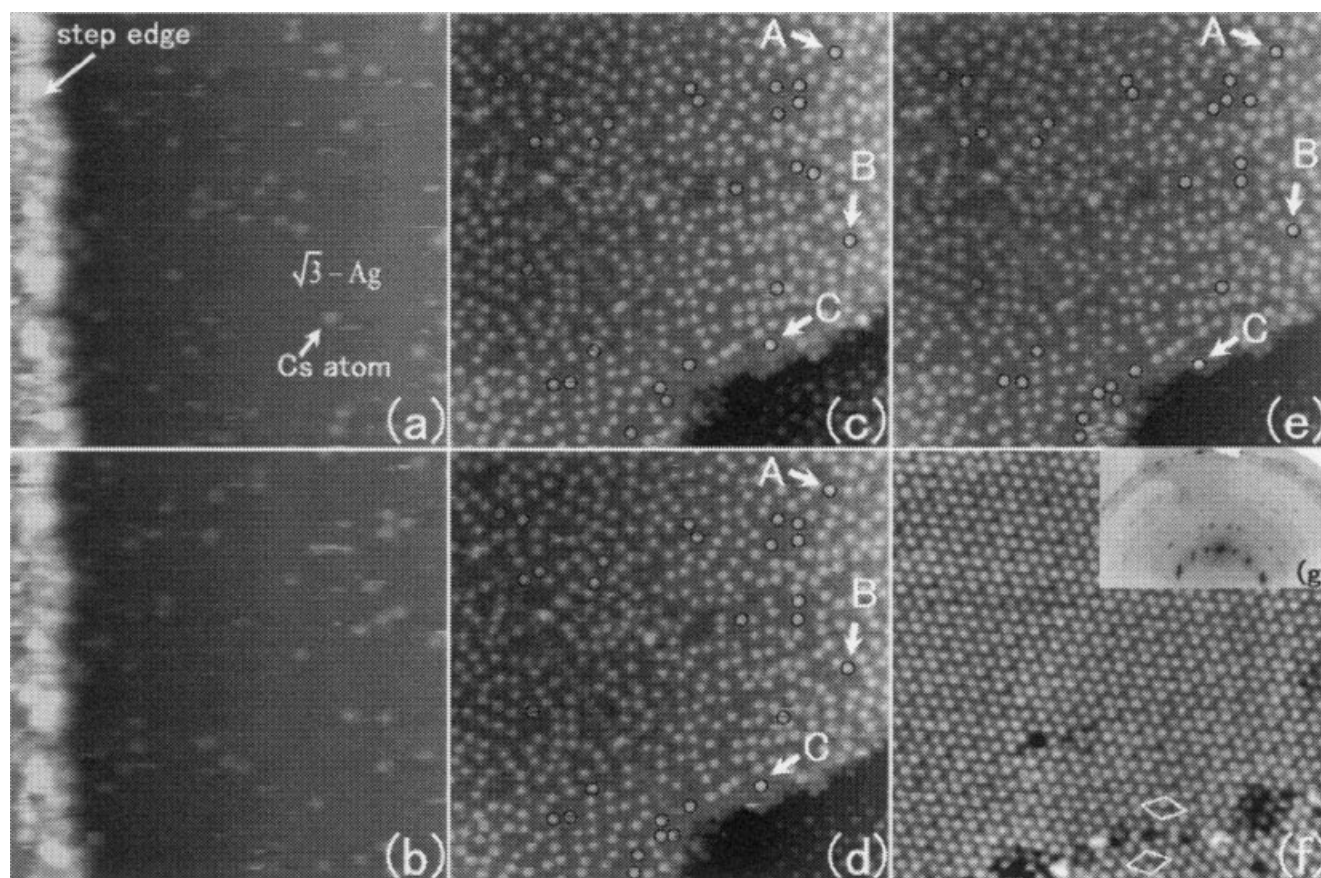


**Figure 1.** Topographic STM images taken at 65 K for Cs adsorptions on the  $\sqrt{3}$ -Ag surface with various coverages. The size of each image is  $30\text{ nm} \times 30\text{ nm}$ . (a,b) The gas-phase image at a Cs coverage of 0.01 ML and the image taken in the same area at an interval of 100 s;  $V_{\text{tip}} = -0.75\text{ V}$ ,  $I_t = 0.75\text{ nA}$ . (c–e) The liquid phase at 0.09 ML coverage with a scanning interval of 150 s;  $V_{\text{tip}} = 2.00\text{ V}$ ,  $I_t = 1.00\text{ nA}$ . (f) The solid phase at 0.14 ML;  $V_{\text{tip}} = 2.00\text{ V}$ ,  $I_t = 0.75\text{ nA}$ . (g) The RHEED pattern after the STM image (f) was taken; incident azimuth is  $[11\bar{2}]$  and the primary electron energy is 14.5 keV.

fact that most of the nearest-neighbour atoms are separated from each other by similar spacing. This is more evident with a Fourier-transformed pattern (not shown here), which shows short-range order in atomic arrangement (details will be published elsewhere). Furthermore, some of the Cs atoms denoted by black circles in Figs 1(c)–1(e) obviously change their positions in successive images. We found three kinds of movement of the atoms in these STM images, as indicated by arrows A, B and C, respectively. Atom A hops back and forth between very close sites; atom B hops to a close site (from (c) to (d)) and then stops moving (from (d) to (e)); atom C stays at a site from (c) to (d) and then hops to a fairly distant site (from (d) to (e)). By continuing to image, other atoms were observed to move too. Thus we consider that the movable atoms should not be limited to those denoted by black circles here; rather, most of the atoms move in a long time scale. But their mobility is so low that most of them seem to be at a standstill in a few successive STM images. The hopping rate of Cs atoms is estimated from these STM images to be  $\sim 0.02$  hops  $\text{min}^{-1}$  and it increases as the Cs coverage decreases. This is a very low hopping rate because of the temperature of 65 K. It is reasonable to believe that at a higher temperature the hopping rate should be much larger. Actually at room temperature we could not obtain STM images like Figs. 1(c)–1(e) because the Cs atoms move around very rapidly on the surface (so it should be a gas phase at room temperature). Thus, because the Cs overlayer exhibits short-range order in atomic arrangement and possesses a low mobility at 65 K, we conclude that it is in a two-dimensional liquid state.

As the Cs coverage is increased to 0.14 ML, the Cs overlayer condenses further into a two-dimensional solid phase, forming the  $\sqrt{21}$ -Cs surface superstructure whose STM image is shown in Fig. 1(f). There are two domains rotated by  $21.78^\circ$  with respect to each other and separated by a domain boundary in the image. Two unit cells of the  $\sqrt{21}$ -Cs surface in the respective domains are denoted by

quadrangles. The unit cell contains three bright protrusions, i.e. three Cs atoms, therefore we make a conclusion that the saturation coverage for the two-dimensional solid phase of the Cs overlayer is  $3/21 = 0.143$  ML.

This  $\sqrt{21}$ -Cs surface structure exists only at low temperature. After Cs atoms of 0.14 ML were deposited on the  $\sqrt{3}$ -Ag surface at room temperature, the RHEED pattern displayed no change; it shows diffraction spots of the  $\sqrt{3}$ -Ag structure only and no existence of the  $\sqrt{21}$ -Cs structure. But, by cooling the sample down to 65 K, the  $\sqrt{21}$ -Cs structure is formed. Figure 1(f) is for the sample made in this way. After this STM observation at 65 K, the RHEED pattern displayed sharp diffraction spots of the  $\sqrt{21}$ -Cs structure as shown in Fig. 1(g), therefore this 'two-dimensional solid' is formed at 65 K by 'freezing' the two-dimensional gas phase at room temperature. It should be noticed here that this  $\sqrt{21}$ -Cs surface structure formed at low temperature is not the same as that formed at room temperature with a much higher coverage.<sup>7</sup> They are different not only in the preparation temperature but also in Cs coverage by more than three times.

A question left here is whether the bright protrusions in Fig. 1 are individual Cs atoms or clusters. Figure 2(a) is an enlarged high-resolution STM image where, in addition to bright and round protrusions, the  $\sqrt{3}$ -Ag substrate is imaged; a unit cell (denoted by a quadrangle) and domain boundary of the substrate of  $\sqrt{3}$ -Ag surface are also identified clearly. We believe that the protrusions in the STM images show mainly the topographical shape because even at high Cs coverage where the  $\sqrt{21}$ -Cs structure is formed the positions of protrusions stay unchanged when we change the polarization of the tip bias. Figure 2(b) shows cross-sections along lines AB and CD in Fig. 2(a), from which the diameter of the round protrusions is estimated to be  $\sim 0.63$  nm. Figure 2(b) also shows that they have approximately the same vertical height. A line profile along line EF across a step edge in Fig. 2(c) is shown in Fig. 2(d), from which, by comparing the monatomic step height, we estimate the height

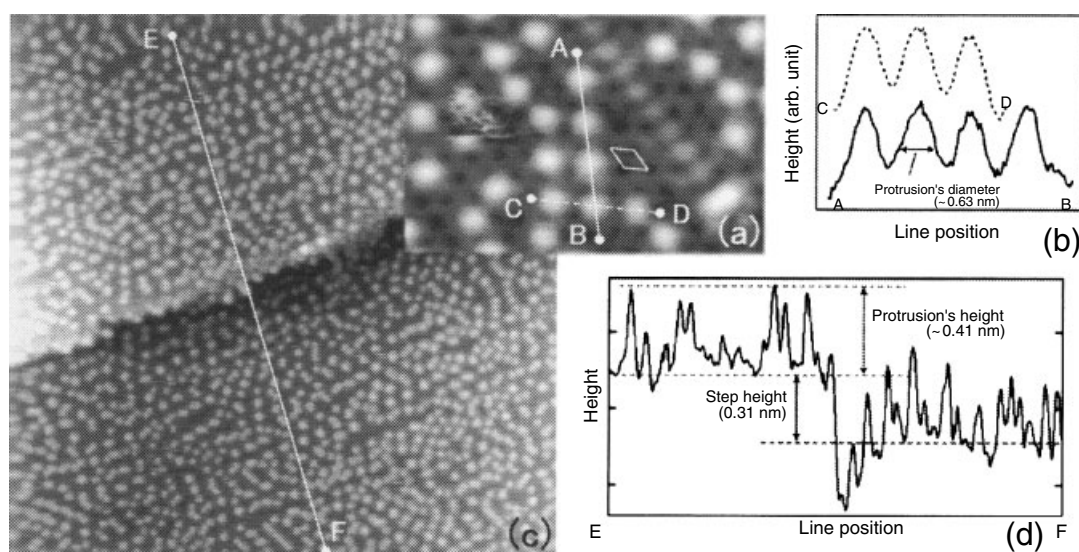


**Figure 2.** Topographic STM images taken at 65 K at a Cs coverage of 0.09 ML for calibrating the size of the bright protrusions: (a) enlarged STM image of size 9 nm  $\times$  6 nm ( $V_{\text{tip}} = 1.50$  V,  $I = 1.00$  nA); (b) profiles along lines AB and CD in (a); (c) STM image of size 42 nm  $\times$  42 nm, taken on an area containing a step edge ( $V_{\text{tip}} = 2.50$  V,  $I = 1.00$  nA); (d) profile along line EF in (c).

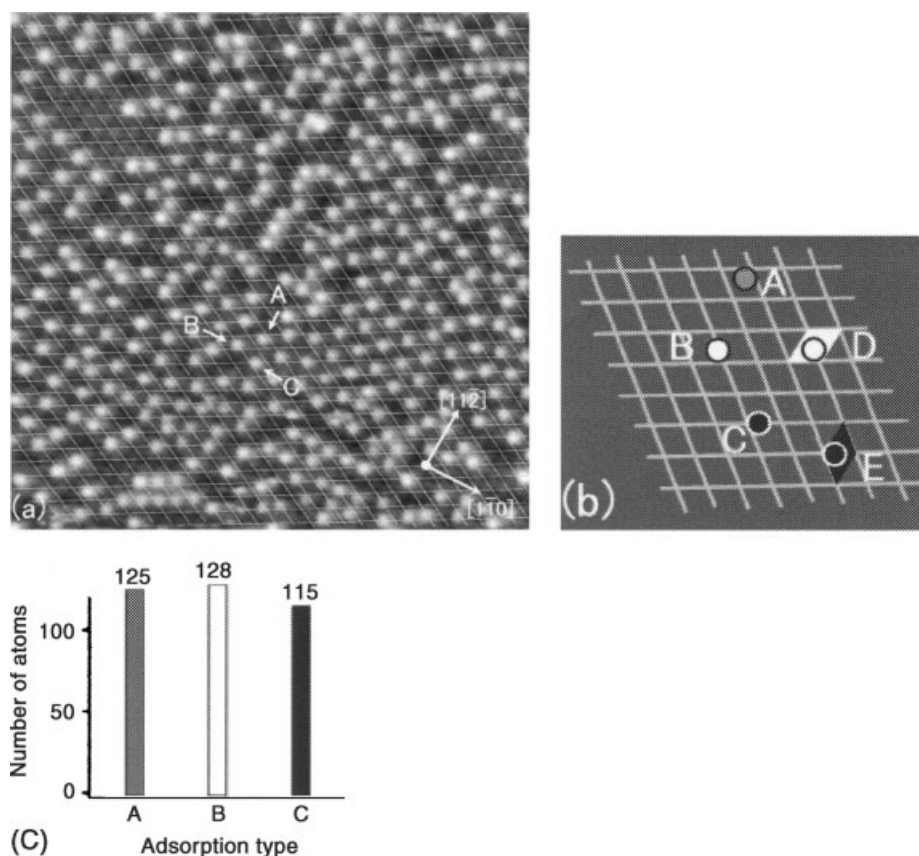


**Figure 3.** (a) Topographic STM image at a Cs coverage of 0.12 ML with a  $\sqrt{3} \times \sqrt{3}$  grid superimposed (20 nm  $\times$  20 nm,  $V_{\text{tip}} = 1.5$  V,  $I = 1.00$  nA). (b) Schematic of Cs adsorption sites on a  $\sqrt{3} \times \sqrt{3}$  grid. (c) Statistics of the Cs adsorption sites.

of the protrusions on terraces to be  $\sim 0.41$  nm. Because the lateral diameter and height are generally imaged in STM to be larger and smaller, respectively, than the real sizes of objects due to a finite size of the very end of an STM tip, the real lateral size of the protrusion is  $< 0.63$  nm and the real height is  $> 0.41$  nm. Because, on the other hand, the ionic and covalent diameters of Cs atoms are 0.34 nm and 0.52 nm, respectively, it is hard to think that one protrusion contains two or more Cs atoms or ions. Considering the fact that the substrate of the  $\sqrt{3}$ -Ag surface does not appear to be destroyed (as shown in Fig. 2(a)), no Ag or Si atoms are released from the substrate to aggregate into such protrusions, therefore we believe that each protrusion corresponds to a single Cs atom. Based on this conclusion, we determined the Cs coverage by counting the densities of protrusions in the STM images.

The short-range order in the atomic arrangement of the Cs overlayer in the liquid state and the long-range order in the solid state suggest that the Cs atoms may have preferred adsorption sites. To find it, we superimpose a  $\sqrt{3} \times \sqrt{3}$  grid on the STM image shown in Fig. 3(a), where the substrate of the  $\sqrt{3}$ -Ag structure can be recognized. The vertices of the grid are located on the centre of Si trimers in a so-called 'honeycomb-chained-triangle' (HCT) model<sup>13</sup> or an 'inequivalent triangle' (IET) model<sup>17</sup> for the  $\sqrt{3}$ -Ag structure. With the reference of the  $\sqrt{3} \times \sqrt{3}$  grid, the adsorption sites of Cs atoms are classed into three types as schematized by A, B and C in Fig. 3(b). Three Cs atoms denoted as A, B and C in Fig. 3(a) are selected as examples.

We count the numbers of each adsorption type, finding that they appear in nearly equal probabilities as shown in Fig. 3(c). To understand this result, two other atoms D and E are illustrated in Fig. 3(b). They occupy the same positions as atom B and atom C with respect to the superimposed  $\sqrt{3} \times \sqrt{3}$  grid, respectively. By regarding atom D with respect to the equivalent  $\sqrt{3} \times \sqrt{3}$  unit cell denoted by the white quadrangle, we find that it is equivalent to atom A. Using atom E, atom C is also found to be equivalent to atom A. Thus, these three types of adsorption sites A, B and C are essentially the same, and all the atoms adsorb on an identical site in the  $\sqrt{3} \times \sqrt{3}$  unit cell. It is worth mentioning that the STM image in Fig. 3(a) contains not only an area of liquid phase but also an area of solid phase (local surface structure of  $\sqrt{21}$ -Cs), and so this finding can be used for constructing the atomic structure of the  $\sqrt{21}$ -Cs surface as discussed below.

In past research on Au and Ag adsorptions on the  $\sqrt{3}$ -Ag surface, Au and Ag atoms were thought to adsorb on the centre of Ag triangles<sup>8–11</sup> or on Si trimers<sup>12</sup> in the HCT or IET models. However, by analysis of Fig. 3 it is revealed that Cs adsorption is evidently a different case in which the Cs atoms sit on a site above the  $H_3$  sites of the second Si layer, as illustrated in Fig. 4(a). We tentatively call it the 'above  $H_3$ ' site.

Although the HCT model was used widely in demonstrating foreign atom adsorption on the  $\sqrt{3}$ -Ag surface, recent research<sup>5,14–16</sup> has found that another model, the IET model,<sup>17</sup> is more reasonable for the atomic structure of the  $\sqrt{3}$ -Ag

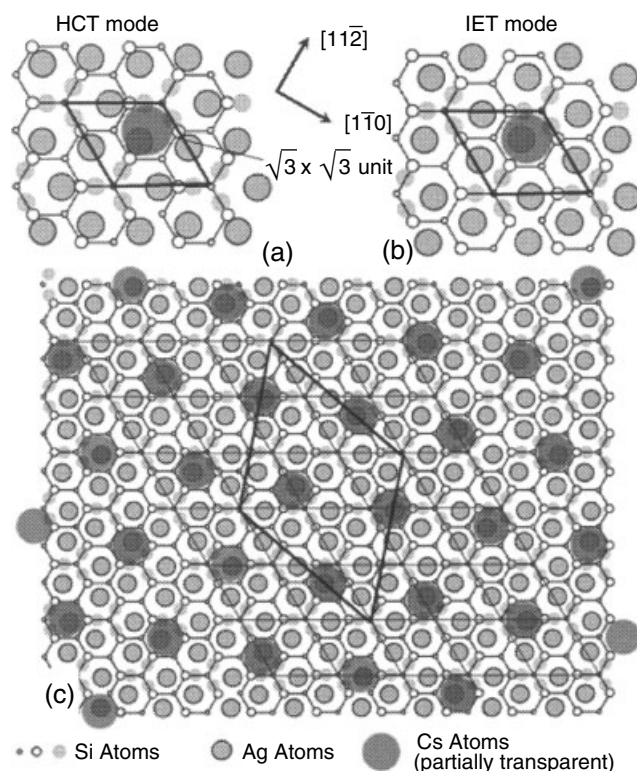


**Figure 4.** Schematics illustrating the Cs adsorption site based on the two atomic structure models of the  $\sqrt{3}$ -Ag surface: (a) on the HCT model; (b) on the IET model; (c) an atomic structure model of the  $\sqrt{21}$ -Cs surface based on the IET model.

surface. We show a schematic in Fig. 4(b) for the Cs atom adsorbing at the 'above  $H_3$ ' site in the IET model. Based on the STM image in Fig. 3 with the finding that Cs atoms sit upon the 'above  $H_3$ ' sites only, we propose an atomic structure model for the  $\sqrt{21}$ -Cs surface in Fig. 4(c) by assuming that the framework of the  $\sqrt{3}$ -Ag substrate is not severely destroyed by the Cs adsorption. The relative positions of Cs atoms in the  $\sqrt{21} \times \sqrt{21}$  unit cell are naturally consistent with those of the three bright protrusions in STM images of the  $\sqrt{21}$ -Cs surface.

The above model of the Cs adsorption site is based mainly on STM observations but we have to mention that with only STM images definite positions of Cs atoms cannot be decided precisely, and we cannot deny the possibility that with Cs adsorption the Ag atoms may change their positions slightly from the original ones in the  $\sqrt{3}$ -Ag structure. Further research, such as x-ray or electron

diffraction, is needed to determine definite positions of the Cs atoms.

## SUMMARY

The initial stage of Cs adsorption on the  $\sqrt{3}$ -Ag surface has been investigated by STM at 65 K. The Cs overlayer can be viewed as two-dimensional matter and conducts two-dimensional gas–liquid–solid phase transitions when the density of Cs atoms is increased. In the two-dimensional gas and liquid phases the Cs atoms are movable. The two-dimensional solid phase is the  $\sqrt{21}$ -Cs surface superstructure that existed only at low temperatures. By estimating the size of bright protrusions in STM images, we find that each protrusion corresponds to a single Cs atom. It is revealed that there are three Cs atoms in a unit cell of the  $\sqrt{21}$ -Cs structure, so that the saturation coverage of Cs for the two-dimensional solid phase is calculated to be 0.143 ML. The Cs atoms on the surface of  $\sqrt{3}$ -Ag are observed to prefer adsorbing on the 'above  $H_3$ ' sites. Based on this conclusion, we propose an atomic structure model for the  $\sqrt{21}$ -Cs structure with the Cs coverage of 0.143 ML.

## REFERENCES

1. Dash JG. *Rev. Mod. Phys.* 1999; **71**: 1737.
2. Strandburg KJ. *Rev. Mod. Phys.* 1988; **60**: 161.
3. Fan WC, Ignatiev A. *Phys. Rev. B* 1988; **37**: 5274.
4. Aruga T, Tochihara H, Murata Y. *Surf. Sci.* 1986; **175**: L725.
5. Matsuda I, Morikawa H, Liu C, Ohuchi S, Hasegawa S, Okuda T, Kinoshita T, et al. *Phys. Rev. B* 2003; **68**: 0854 507.
6. Hasegawa S, Tong X, Takeda S, Sato N, Nagao T. *Prog. Surf. Sci.* 1999; **60**: 89.
7. Liu C, Matsuda I, Morikawa H, Okino H, Okuda T, Kinoshita T, Hasegawa S. *Jpn. J. Appl. Phys.* 2003; **42**: 4659.
8. Nogami J, Wan KJ, Lin XF. *Surf. Sci.* 1994; **306**: 81.
9. Tajiri H, Sumitani K, Yashiro W, Nakatani S, Takahashi T, Akimoto K, Sugiyama H, et al. *Surf. Sci.* 2001; **493**: 214.
10. Tong X, Sugiura Y, Nagao T, Takami T, Takeda S, Ino S, Hasegawa S. *Surf. Sci.* 1998; **408**: 146.
11. Aizawa H, Tsukada M. *Phys. Rev. B* 1999; **59**: 16.
12. Ichimiya A, Nomura H, Horio Y, Sato T, Sueyoshi T, Iwatsuki M. *Surf. Rev. Lett.* 1994; **1**: 1.
13. Takahashi T, Nakatani S, Okamoto N, Ichikawa T, Kikuta S. *Jpn. J. Appl. Phys.* 1988; **27**: L753.
14. Nakamura Y, Kondo Y, Nakamura J, Watanabe S. *Phys. Rev. Lett.* 2001; **87**: 156 102; *Surf. Sci.* 2001; **493**: 206.
15. Sasaki N, Watanabe S, Tsukada M. *Phys. Rev. Lett.* 2002; **88**: 046 106; *Surf. Sci.* 2001; **493**: 206.
16. Kakitani K, Yoshimori A, Aizawa H, Tsukada M. *Surf. Sci.* 2001; **493**: 200.
17. Aizawa S, Tsukada M, Sato N, Hasegawa S. *Surf. Sci.* 1999; **429**: L509.